Congreso Nacional de Control Automático 2013
Ensenada, Baja California, Mexico, Octubre 16-18, 2013

AMCA

Energy Management Strategies under Uncertainties for Electric Vehicles

Ilse Cervantes
Hybrid Systems Laboratory, Applied Mathematics Division, IPICyT,
Camino a la Presa San José 2055 Col. Lomas 4ta 78216
San Luis Potosí, S. L. P., México. Email: ilse@ipicyt.edu.mx;
J. Morales-Morales
Hybrid Systems Laboratory, Applied Mathematics Division, IPICyT.
Email: josefa.morales@ipicyt.edu.mx
Ulises Cano
Fuel Cells and Hydrogen Group. Institute for Electrical
Research (IIE). Email: ucano@iie.org.mx

***Abstract*—In this paper, we analyze the limitations that imposes the presence of uncertainty in the design of energy management strategies for FC (fuel cell) electric vehicles. Using a electric power source constituted by a hydrogen fuel cell and a battery bank, the fuel consumption minimization problem is analyzed in the presence of parametric uncertainty. The conditions that ensure that the nominal solution matches the real (uncertain) solution are clearly stated and it is shown that the presence of bounded uncertainty limit the set of admissible solutions. By observing that any finite energy source will also limit the feasible solutions of the optimization problem, a supervisory control is designed to face such limitations. Moreover, a cascade control is proposed to face uncertainties in the current tracking task of the converters. Numerical simulations provide evidence of the advantages and features of the proposed strategy.**

***Keywords*—Energy management, Robust optimization.**

I. Introduction

Nowadays fossil fuels are largely consumed for electric generation and vehicle propulsion[1]. Along with fuel consumption, there is a proportional rise of the levels of environmental pollution therefore some solutions based on renewable energy have been proposed [1]-[8]. Electric propulsion of vehicles constitutes an option widely studied to design zero-emissions transportation [1]-[8]. Electric vehicles through the use of modern electric storage systems (ESS) have shown its reliability and technical feasibility [3]. Among known technologies, Proton Exchange Membrane Fuel Cells (PEMFC), constitute the most suitable solution to extend the vehicle autonomy with zero emissions; furthermore their tank can be filled in short periods of time, as conventional vehicles do (see [2]). However, the technical feasibility and safety of the use of FC in practical applications must be still demonstrated [3]. In order to provide such technical evidence, a variety of authors has proposed design criteria for the power propulsion system [12]-[16] as well as energy management strategies (EMS) [4]-[8], [11], [17],[18]. Most of these EMS can be categorized as i) optimization based and/or ii) heuristic-rule based. In either one, the objective is to reduce the fuel consumption while guaranteeing the accomplishment of security and performance restrictions on the ESS and the FC.

An advantage of the optimization-based strategies is that their solution can be called ”minimal” and that they have the back-up of formal results that allows its application in a wide number of vehicles. On the other hand, heuristic based strategies generally lack of theoretical support but they are simple and can be applied in real-time. Its application has been shown successfully in a variety of vehicular systems [8], [19]. Among the optimization-based strategies it is worthy noticing the following works. In [4], the restrictions of the optimization problem are fixed according to a maximum FC efficiency. The strategy takes into account also important restrictions on the rate of change of the FC delivered power, which ensures that the FC does not flood nor dry. However as the authors state in [5], operation of the cell at the maximum efficiency cell zone, over-dimensions the size of the cell and its power generation is not completely exploited. On the other hand, in [6] a two-stage energy management control is proposed that takes into account the FC longevity. Based in a discrete-time model of the propulsion system, the Pontryagin´s Minimization principle is used to reformulate a full-driving-cycle optimization problem into an instantaneous optimization problem. The problem of computing unknown multipliers of the objective function is solved using a statistical model over all possible driving cycles. The authors show the feasibility of the application trough numerical simulations.

In spite of all these works above constitute important advances, still some questions regarding the effect of uncertainty in optimized EMS are unsolved. The aim of this paper is along these lines. In particular, in this paper we analyze the effect of parametric uncertainty in the fuel consumption minimization problem in an electric power-train constituted of a bank of batteries and a PEMFC. To this end, we

depart of a unknown traction model and unknown objective function and driving cycle, to analyze the limitations of finding the "real" optimum. In particular, if the nominal value and an upper bound of the parameter uncertainty are available, the conditions that ensure the coincidence of the nominal and real optimal solution are clearly stated. To overcome the limitations that inevitably impose the design of the power-train in the existence of the optimal solution, a robust supervisory-cascade control is proposed to ensure the availability of energy and the required power in the hybrid power-train. The proposed strategy has the advantage of being feasible to implement in real-time applications, since is based in discrete-time description and can be found analytically.

This paper is organized as follows: The models and the uncertain optimization problem are introduced in Section II. The existence and the computation of the optimal solution is given in Section III the supervisory control is analyzed in Section IV.Numerical simulations are shown in Section V, and finally, Section VI summarizes the main contribution of this paper and presents some conclusions.

II. System Description and Problem Statement

Let us consider an electric vehicle with the power-train given in Figure 1. The vehicle uses energy from a PEMFC and/or from a battery bank with the help of two DC-DC links, one for each energy source. Such configuration allows the control of the shared power as well as its rate of change.

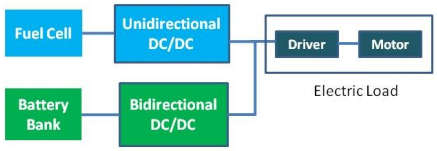

Fig. 1. Electric Power-train.

The electric power demanded by the vehicle is dependent of various factors: i) the vehicle dynamics (*i.e.* rolling resistance, gravitational and aerodynamical forces, etc.) ii) the efficiency of the movement transmission given by the mechanical design of the vehicle (η_t), iii) the efficiency of the converters (η_c), the motor efficiency (η_{motor}) and the efficiency of the battery bank and FC (η_{source}) and finally iv) the driving conditions.

The schematic diagram of the power demand is given in Figure 2. In this paper, *we will assume that such power demand is known at every (present) time and that no predictive knowledge of the driving cycle is available*. Notice that such assumption implies the knowledge of the current demand at every time k and that the results of the energy management strategy are valid even in presence of uncertain vehicle dynamics. The objective of the power management strategy is to minimize the fuel consumption by choosing an appropriate power split among the FC and the battery

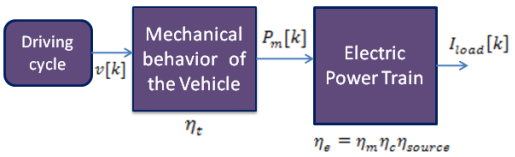

Fig. 2. Power Demand.

bank. It is known that the hydrogen consumption (Δm_{H_2}) is proportional to the current delivered by the fuel cell (I_{FC}) [7], [8]; that is

$$\Delta m_{H_2} = -\frac{N M_{H_2} I_{FC}}{2F} \tag{1}$$

where N is the number of cells in the stack, M_{H_2} is the molar mass of H_2 and F is the Faraday constant. Moreover since at every time the current supplied by the battery bank I_B and by the fuel cell must satisfy the following:

$$I_{load}[k] = I_B[k] + I_{FC}[k] \tag{2}$$

where $I_{FC}[k] > 0$ and $I_{load}[k]$ is the current demanded by the load, it is clear that we can introduce a convex parametrization in (2) to propose a suitable objective function that attain the minimization objective. That is, in view of Eq. (2), let us define the parameter β with $0 \leq \beta \leq 1$, such that if $\beta = 1$ all the current required by the load is provided by the batteries and if $\beta = 0$ all the current is provided by the fuel cell; while for $0 < \beta < 1$, the current is provided by both sources. Using such parametrization the battery and FC currents are given by $I_B[k] = \beta I_{load}[k]$, $I_{FC}[k] = (1-\beta) I_{load}[k]$ and the minimization problem can be formulated as follows,

$$\min_{\beta} J = c(1-\beta)^2 (I_{load}[k])^2 \tag{3}$$

with $c > 0$ a constant. Observe that (3) is proportional to the quadratic hydrogen consumption and it has been chosen as a suitable convex function of parameter β to guarantee the existence of the optimized solution [20]. The minimization problem is subjected to the following restrictions:

$$SOC[k] - SOC_{max} \leq 0 \quad \text{with} \quad SOC_{max} \leq 1 \tag{4}$$

$$SOC_{min} - SOC[k] \leq 0 \quad \text{with} \quad SOC_{min} > 0 \tag{5}$$

$$SOC[k+1] = SOC[k] - c_1 I_B[k] \quad \text{with} \quad c_1 > 0 \tag{6}$$

$$P_{FC}[k] - P_{FCmax} \leq 0 \quad \text{with} \quad P_{FCmax} > 0 \tag{7}$$

$$P_{FCmin} - P_{FC}[k] \leq 0 \quad \text{with} \quad P_{FCmin} > 0 \tag{8}$$

$$\Delta P_{FC}[k] - \Delta P_{FCmax} \leq 0 \quad \text{with} \quad \Delta P_{FCmaxn} > 0 \tag{9}$$

$$\Delta P_{FCmin} - \Delta P_{FC}[k] \leq 0 \quad \text{with} \quad \Delta P_{FCmin} < 0 \tag{10}$$

where SOC is the state of charge of the battery bank, P_{FC} is the power supplied by the Fuel Cell and ΔP_{FC} is the rate

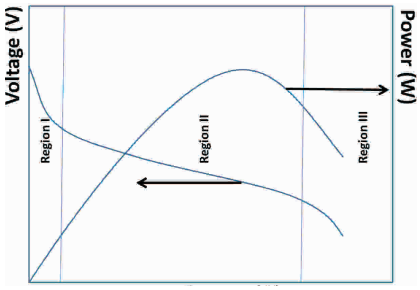

Fig. 3. Schematics of a typical PEMFC polarization curve

of change on P_{FC}. Notice that a discrete time k is used to describe the time evolution of the system.

In order to express restrictions (4)-(10) as function of β, consider the following arguments. The polarization curve can be used to express the voltage of the fuel cell as a function of the its current (*i.e.* $V_{FC} = g(I_{FC})$). In general, a polarization curve is comprised of three regions (See Figure 3). A first one, at low current and high voltages, where current losses are related with the required energy to initialize the reaction (open-circuit zone). A second one, where current losses are mainly attributed to the Ohmic resistance of the electrolyte resistivity and the external resistance of electrodes and connections (linear region), and a third one, located at high current and low voltages, where the behavior is limited by the mass transfer rate (depletion zone). For safety reasons, it is reasonable to exclude depletion and open-circuit zones from the FC operation; therefore, FC power can be expressed as:

$$\begin{aligned} P_{FC}[k] &= I_{FC}[k](-a_1 I_{FC}[k] + b_1) \\ &= (1-\beta)I_{load}[k](-a_1(1-\beta)I_{load}[k] + \\ &+b_1) \end{aligned} \tag{11}$$

The restrictions (4)-(10) can be rewritten in function of β as follows

$$f(\beta;\gamma) \leq 0 \tag{12}$$

where

$$f(\beta;\gamma) = \begin{bmatrix} \frac{SOC_{max}-SOC[k]}{\gamma_1 I_{load}[k]} - \beta \\ \beta + \frac{SOC_{min}-SOC[k]}{\gamma_1 I_{load}[k]} \\ (1-\beta)I_{load}[k][-\gamma_2(1-\beta)I_{load}[k] + \gamma_3] - \gamma_4 \\ (1-\beta)I_{load}[k][+\gamma_2(1-\beta)I_{load}[k] - \gamma_3] + \gamma_5 \\ \beta - 1 \\ -\beta \end{bmatrix} \tag{13}$$

with $\gamma = [c_1, a_1, b_1, \overline{P}_{FCmax}, \overline{P}_{FCmin}]^T$ where γ_i with $i = 1...6$, be the elements of γ and $\leq$ denote element-wise inequality.Where

$$\overline{P}_{FCmin} = \max\{P_{FCmin}, P_{FC}[k-1] + \Delta P_{FCmin}\}$$

$$\overline{P}_{FCmax} = \min\{P_{FCmax}, P_{FC}[k-1] + \Delta P_{FCmax}\}$$

and $P_{FC}[k-1]$ is given by (11). Notice that the last two entries of f account for $0 \leq \beta \leq 1$. Let us denote the nominal value of the parameter vector γ as $\overline{\gamma}$ and the maximum allowable uncertainty bound as $\Delta\gamma_{max}$. The restrictions

$$f(\beta;\overline{\gamma}) \leq 0 \tag{14}$$

constitute the nominal value of restrictions (12). Let us denote as Uncertain Fuel Economy Minimization problem (UFEMP) the minimization of (3) subjected to (12) and Nominal Fuel Economy Minimization problem (NFEMP), the minimization of (3) subjected to (14).

A. Problem Statement

Consider a given vehicle design with a traction system given in Figure 1.

Problem 1:Compute the solution of the NFEMP and establish conditions for the this solution to match the solution of the UFEMP.

Problem 2: Establish an energy management policy that ensures the current feeding to the load and performance of the traction system in spite of parametric bounded uncertainty.

III. The solution of the NFEMP and the uncertain optimization problem

Let us assume the existence of the following two sets:

$$\Omega^{uncertain} = \{\beta | f(\beta;\gamma) \leq 0\} \tag{15}$$

$$\Omega^{nom} = \{\beta | f(\beta;\overline{\gamma}) \leq 0\} \tag{16}$$

where $\Omega^{uncertain}$ and Ω^{nom} are the feasible sets of the real and nominal restrictions. Notice that is reasonable to assume the existence of such sets, otherwise the solutions of the nominal and uncertain constrained minimization problem do not exist. Let us denote such solutions as $\overline{\beta}_{min}$ and β_{min} respectively.

Let us compute the solution of the NFEMP ($\overline{\beta}_{min}$).There exist in the literature a variety of numerical methods for the computation of the solution; however, the relative simplicity of the problem allows us to illustrate the solution as a function of the demanded current $I_{load}[k]$. In view of Eq. (13), it is clear that the restrictions of both, the battery and the fuel cell are dynamical, changing at every instant k. Let f_i, $i = 1...6$, be the elements of (13). Notice that restriction $f_1 \leq 0$ is only active while the battery is charging. On the other hand, since $f_2 \leq 0$ is related with the minimum level of SOC it must be monitored continuously. Observe that such restriction depends inversely of the demanded current $I_{load}[k]$ and that the maximum value of β is given by the distance $SOC_{min} - SOC[k]$. That is, the larger SOC level, the larger β is allowed for a given current demand.

Restrictions $f_3 = 0$ and $f_4 = 0$ can be rewritten as:

$$-\overline{\gamma}_2 z^2 + \overline{\gamma}_3 z - \overline{\gamma}_4 = 0 \tag{17}$$

$$-\overline{\gamma}_2 z^2 + \overline{\gamma}_3 z - \overline{\gamma}_5 = 0 \tag{18}$$

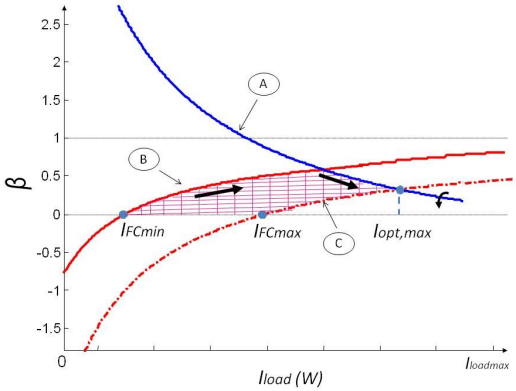

Fig. 4. Feasible region for optimization

Notice that the solutions of (17)-(18) depends only on FC parameters and therefore, they can be computed off-line. Before computing such solution it is worth noting that most fuel cells display a quadratic behavior of the derived power upon the current; that is, the same power can be obtained with two different currents (see Figure 3). It is known that the depletion zone is usually avoided because the cell floods, leading to a FC malfunction. In view of the arguments above, it is possible to establish that for most fuel cells $\gamma_3^2 > 4\gamma_2\gamma_4$ and both solutions of (17)- (18) are real; however, the high current solution is avoided because it belongs to the depletion zone.

In this way, let us consider the low current solutions of (17)-(18), these are:

$$z_{min} = \frac{-\overline{\gamma}_3 + \sqrt{\overline{\gamma}_3^2 - 4\overline{\gamma}_2\overline{\gamma}_5}}{-2\overline{\gamma}_2} \tag{19}$$

$$z_{max} = \frac{-\overline{\gamma}_3 + \sqrt{\overline{\gamma}_3^2 - 4\overline{\gamma}_2\overline{\gamma}_4}}{-2\overline{\gamma}_2} \tag{20}$$

Figure 4 displays these curves denoted as B and C respectively. Observe that the solution of the nominal optimization problem is only feasible in the shaded region, where restrictions from the battery and the fuel cell are satisfied.

From Figure 4 it is also possible to observe the existence of a maximum current demand $I_{opt,max}$ for which the power share is feasible. The solution moves along line B (minimum FC power) until the battery discharges considerably for curve A to intersect B. At this point the power split moves along the battery restriction, curve A, until it intersects the curve of the maximum FC power (curve C) at $I_{opt,max}$. Notice that the distance $I_{opt,max} - I_{FC,max}$ where $I_{FC,max}$ is the maximum current that can be extracted to the fuel cell, depends on battery SOC and beyond this point, the only choice is to use the FC as sole energy source. In general $I_{opt,max} \geq I_{FC,max}$ being $I_{opt,max} = I_{FC,max}$ only when the battery attains its minimum level (recall that curves A,B,C are time-varying). Notice also that if the SOC level is high, the solution $\beta = 1$ (the unconstrained solution) may be feasible, and nominal and real solutions match.

***Remark** 1:* It is clear at this point, that the design restrictions (16) naturally impose limitations to the optimization-based energy management strategy and that such strategy alone cannot be applied directly. Therefore in this paper we propose the use of a supervisory control (see Figure 5) that allows the correct operation of the propulsion system, even when optimization is not possible.

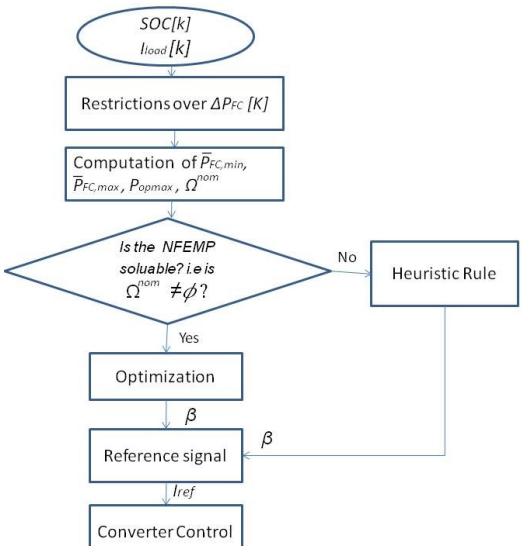

Fig. 5. Proposed energy management strategy.

A. Connections with the solution of the UFEMP

At this point the solution of the NFEMP $\overline{\beta}_{min}$ has been found, but still is not clear if $\overline{\beta}_{min}$ will satisfy the real restrictions (12); that is , two questions still remain open: i) How the nominal parameter vector $\overline{\gamma}$ can be chosen to satisfy the (uncertain) real restrictions? and ii) When the solutions of the NFEMP and UFEMP are the same? (*i.e.* $\overline{\beta}_{min} = \beta_{min}$). In order to answer these questions, firstly notice that $\Omega^{uncertain} \cap \Omega^{nom} \neq \emptyset$ is a necessary condition for $\overline{\beta}_{min} = \beta_{min}$ otherwise the solutions may belong to two different and disconnected sets. Let

$$\partial\Omega^{nom} = \{\beta | f(\beta; \overline{\gamma}) = 0\} \tag{21}$$

***Remark** 2:* If $\Omega^{uncertain} \supset \Omega^{nom}$, $\beta_{min} \in \Omega^{nom}$ and $\beta_{min} \notin \partial\Omega^{nom}$ then the solutions of the NFEMP and UFEMP coincide.

To see clearly this point, let us recall that β is scalar; therefore, restrictions (12) and (14) can be reduced to a maximum and minimum restrictions over β as follows:

$$\begin{aligned} \Omega^{uncertain} &= \{\beta | \beta \leq \beta_{real,max} \wedge \beta \geq \beta_{real,min}\} \\ \Omega^{nom} &= \{\beta | \beta \leq \beta_{nom,max} \wedge \beta \geq \beta_{nom,min}\} \\ \partial\Omega^{nom} &= \{\beta = \beta_{nom,max} \wedge \beta = \beta_{nom,min}\} \end{aligned}$$

with

$$\beta_{max,max} \leq \beta_{real,max} \leq \beta_{max,min}$$

$$\beta_{min,max} \leq \beta_{real,min} \leq \beta_{min,min}$$

derived from the uncertainty bound $\Delta\gamma_{max}$ and the continuity of (12). If

$$\beta_{nom,max} = \beta_{max,min} \tag{22}$$

$$\beta_{nom,min} = \beta_{min,max} \tag{23}$$

then $\Omega^{uncertain} \supset \Omega^{nom}$. In this case, β_{min} can be found solving the NFEMP, since its solution coincides with the unconstrained solution of the nominal system given that $\beta_{min} \in \Omega^{nom}$ and $\beta_{min} \notin \partial\Omega^{nom}$. However if $\beta_{min} \in \partial\Omega^{nom}$ the solution of the NFEMP becomes $\beta_{min,max}$ or $\beta_{max,min}$ while the solution of UFEMP still is the one of the unconstrained solution of the nominal system. That is, irrespectively of the amount of uncertainty, there always exists a region where both solutions do not coincide, such region occurs in a neighborhood of the estimated value of γ (γ_{est}), given the continuity of (12). The larger the uncertainty, the larger this region is. Moreover, there exist a maximum uncertainty bound such that the real and nominal solutions coincide (i.e. $\beta_{nom,max} \leq \beta_{nom,min}$) beyond this point, solving the optimization problem is not worthy.

***Remark** 3:* Notice that the definition of the nominal values (22)-(23) guarantee the satisfaction of the real restrictions and that $\overline{\gamma}$ can be computed numerically using (12) with an estimated value of γ and the uncertainty bound $\Delta\gamma_{max}$.

IV. Supervisory Control

As stated in Remark 1, the design of the propulsion system inherently limits the optimized values of β (see Figure 4); therefore, we propose an heuristic-based strategy for such cases(see Figure 5). For $I_{load}[k] < I_{FC,min}$ two choices are possible, if the battery SOC is sufficiently high, it is reasonable to use only the battery since our objective is to save as much fuel as possible. However, this choice can not be made if the battery attains its minimum value. In this case, the fuel cell must provide all the power. On the other hand, as stated above, once $I_{load}[k] > I_{opt,max} = I_{FC,max}$ the only choice available is to use the FC alone, while for charging or regenerative breaking mode, restriction (4) must be taken into account. The modes of the supervisory control proposed in this paper are stated in Table I.

Tabla I
Modes of the supervisory control

Mode	β	*Conditions*
1	1	$I_{load}[k] \in [0, I_{FC,min})$ and $SOC[k] \geq SOC_{min}$
2	0	$I_{load}[k] \in [0, I_{FC,min})$ and $SOC[k] < SOC_{min}$
3	$\overline{\beta}_{min}$	$I_{load}[k] \in [I_{FC,min}, I_{opt,max}]$
4	0	$I_{load}[k] \in (I_{opt,max}, I_{FC,lim})$and $SOC[k] < SOC_{min}$
5	reg	$I_{load}[k] \leq 0$ and $SOC[k] < SOC_{max}$
6	$drop$	$I_{load}[k] \leq 0$ and $SOC[k] \geq SOC_{max}$

In this table, "reg" accounts for the regeneration mode and "drop" for the energy dropping mode (*i.e.* when the energy from the regenerative braking cannot be stored and the excess must be dropped); moreover $I_{FC,lim}$ is the limit of operation of the FC. It is worthy noticing that the supervisory control is well defined, since no concurrence of modes can be given and since a control action is always specified for any I_{load}. Moreover, the stability of the supervisory control is guaranteed by the following facts: i) no chattering can occur given the discrete-time nature of the control, ii) the values of β are upper and lower bounded iii) the rate of change of β is also upper and lower bounded. ii) and iii) guarantee that the the trajectories described by the supervisory control are invariant [10] in $0 \leq \beta \leq 1$.

The structure of the supervisory control can be observed in Figure 6. Notice that once the value of β is known, a current reference can be computed using the demanded current and expressions $I_B[k] = \beta I_{load}[k]$ and $I_{FC}[k] = (1-\beta)I_{load}[k]$ to compute the current sharing.

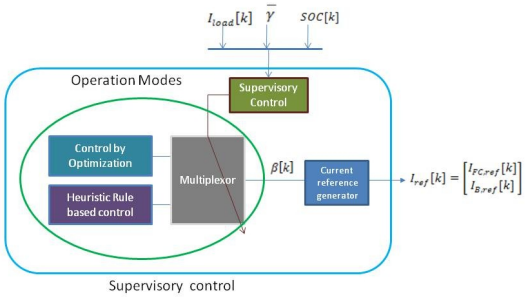

Fig. 6. Supervisory control structure.

Once the reference currents have been computed, the following step is to track them using a cascade control as depicted in Figure 7. To choose a suitable controller for this

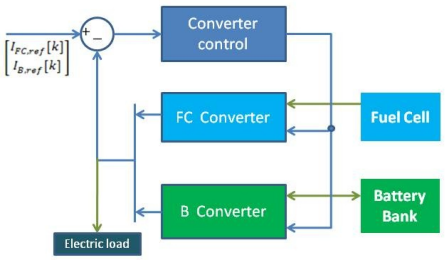

Fig. 7. Structure of the current control.

task, notice that convergence rate of the current controller may impact adversely on fuel economy of the power train, since slow control actions may lead to suboptimal solutions, making useless the optimization stage of supervisory controller. To avoid this limitation , piece-wise-constant or hybrid are better choices that averaged model-based controllers. In this work a hybrid current control is applied [21].

If the converter dynamics is sufficiently fast, the stability of the cascade control can be analyzed as being decoupled; that is, as time-invariant system (regulation) instead as a time-varying one (time-varying tracking). As discussed above, hybrid controllers are more suitable to this task since it is

known that its rate of convergence is not limited by averaged (slow) description of the system.

The robust practical controllability or robust practical stabilizability of the current regulation is studied in [21] departing from a piece-wise model of the converter. In this reference, the conditions over uncertainty to guarantee the stability of the current are explicitly given. Moreover, the controller in [21] guarantee not only fast convergence (the current is followed in n+1 switchings, where n is the number of inductors); but also, a maximum current ripple. Such characteristic is especially convenient for fuel cells, since it is known that large current ripple lead to FC malfunction. If converter settle time is sufficiently low, the stability analysis in [21] can be applied directly to conclude that the robust tracking of the current reference with a maximum current ripple (observe that is the maximum, and not the minimum ripple the one of interest). We illustrate the implementation of this controller in the following section.

V. Illustrative Example

The objective of this section is to evaluate robustness and performance of the proposed control strategy as well as illustrate the implementing procedure of the proposed controller above. To this end, simulations in a vehicle system are performed with the next parameters;$P_{FC,min} = 0W$,$P_{FC,max} = 2800W$,$a_1 = 0.25V/A$,$b_1 = 80V$,$c_1 = 6.914e-5(1/A)$,$c = 1e-5$,$SOC_{min} = 0.25$,$SOC_{max} = 1$,$V_{load} = 200V$,$\Delta P_{FC,min} = -2800W$,$\Delta P_{FC,max} = 2800W$,$\eta_t = 0.9$,$\eta_e = 0.77$,$c_r = 0.014$,$c_d = 0.5$,$A_f = 3.225m^2$,$m_v = 1000Kg$,$r_w = 0.2651$,where c_r rolling coefficient, c_d drag coefficient, A_f frontal area, m_v vehicle mass, φ gear ratio, r_w wheel radius. The converters used are: i) a boost converter for the FC and ii) a bidirectional boost converter for the battery. Through numerical simulations we are interested in i) evaluating the performance of the supervisory control and analyzing the differences of the UFEMP and NFEMP as a function of the uncertainty bounds, ii) analyzing the effect of parameter $\overline{P}_{FC,min}$ on the fuel economy, iii) contrasting our findings for different driving cycles and iv) giving evidence of the applicability of the current control.

A. Results and discussion

As a first step in analyzing the supervisory control, we implement algorithm in Figure 5. At every discrete time k, computation of the power bounds $\overline{P}_{FC,min}$, $\overline{P}_{FC,max}$ must be performed depending on battery SOC. The fuel economy, as a function of parameter $\overline{P}_{FC,min}$ for City II and New European driving cycle under the next cases: i)is the no uncertainty, ii) $\Delta\gamma_2 = -0.125$,$\Delta\gamma_5 = 560$,$\Delta\gamma_1 = 0$,$\Delta\gamma_3 = 0$,$\Delta\gamma_4 = 0$, while iii)$\Delta\gamma_2 = -0.225$,$\Delta\gamma_5 = 2240$,$\Delta\gamma_1 = 0$,$\Delta\gamma_3 = 0$,$\Delta\gamma_4 = 0$. In all cases the initial value of $SOC = 1$.

The fuel economy as a function of parameter $\overline{P}_{FC,min}$ for European (NEDC) [22] and City II Driving Cycle under different uncertainty bounds is shown in Figure 8 and 9. The fuel economy is calculated as follows:

$$FuelEconomy = (H_{2FC} - H_{2EMS})/H_{2FC} \qquad (24)$$

where H_{2FC} is the consumed fuel by using only the Fuel Cell, H_{2EMS} is the consumed fuel by using proposed EMS and two energy sources (Fuel Cell and Battery). From observing in Figure 8 it is clear that for low $P_{FC,min}$ the fuel economy is high. In this cases, the region where optimization is feasible is large, being the largest at $P_{FC,min} = 0$, therefore this region is very susceptible to uncertainty. It can be observed that the real economy is always larger than the uncertain cases (region 1); however this not the region 2. In this case the feasible region for optimization is narrower for the real parameter case, being the narrowest when $P_{FC,min} = P_{FC,max}$;that is, for the proposed strategy, the heuristic rules play more active role in the vehicle performance that optimization. It can be observed that the proposed strategy has the worst performance for curve (i) that when uncertainty is present.

Why in this cases the effect of the uncertainty is so beneficial?, The reason reside in the feasibility region of the nominal optimization problem, reaching for the Figure 8 almost the maximum economy possible for the scenario (ii). These observations can also be performance for New European Driving Cycle (Figure 9)however in this case the shorter duration of the cycle (200s) leads to economy to be more sensitive to variatios.

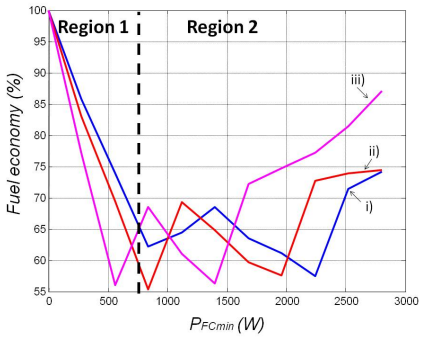

Fig. 8. Fuel Economy as a function of uncertainly bound. European driving cycle.

From the observations above it can be concluded that the uncertainty has an important effect on overall economy. As the set Ω^{nom} becomes narrower, the effect of the uncertainty is more significant. Notice that as uncertainty increases, the difference between UFEMP and NFEMP become more significant (region 1 in Figure 8 and 9). In this point is clear that the designer can evaluate the pertinence of solving the optimization problem in view of the confidence of the estimated parameters, since as discussed above, there exist a maximum upper bound on the uncertainty such that solutions of UFEMP and NFEMP intersect.

B. Evaluation of the supervisory-cascade performance

Due to converter-design considerations, usually the nominal frequency $(1/RC)$ is small compared to the design-

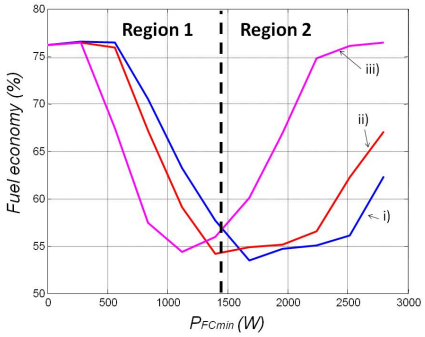

Fig. 9. Fuel Economy as a function of uncertainly bound. City II driving cycle.

switching frequency (f_s); therefore, the output voltage remains constant for short times ($\mathcal{O}(1/f_s)$). Under this condition, it can be seen that inductor current evolves describing piecewise linear trajectories. In particular, when both sources are providing current, each one of the boost converters can be described by the integrator approximation given by $m_{j_{off}} = \frac{E_j - V_{load}}{L_j} \geqslant 0$, and $m_{j_{on}} = \frac{E_j}{L_j} \leqslant 0$, where $j = 1, 2$ (*i.e.* the number of sources is 2). Such approximation is used to design the hybrid current controller. In this case, it is clear that practical stabilizability of the converter can be achieve regardless the uncertainty bound as long as the sign is preserved (see [21] for details). Notice that such uncertainty may arise by the changing voltage of the FC and(or) battery bank, or an inexact value of converters parameters (i.e. inductors, load charge or capacitance).

In this example $\Delta m_{j_{off}} < 4.5$ and $\Delta m_{j_{on}} < -7$ has been chosen. Using this approximation the following step is defining a maximum current ripple, this has been fixed with the help of design criteria as $0.05 \max I_{load}$ (10% of the mean value of I_{load}). Figure 10 shows the time evolution of the split power parameter β and the currents extracted to the FC and battery bank. It is possible to observe that the controller is able to track the reference successfully, guaranteeing the fuel economy of the supervisory stage.

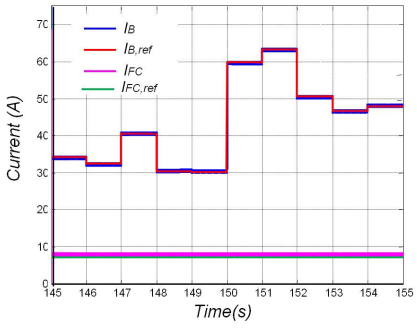

Fig. 10. Time evolution of the converter. City Cycle II driving cycle.

VI. Conclusions

In this work, the role of uncertainty in a optimized-based EMS is analyzed. It is stated that in presence of bounded uncertainty the restrictions of the system may be satisfied but inevitable differences between the solutions of real and uncertain problems arise. The conditions for this discrepancy of solutions are clearly stated. Moreover, it is stated that in order to face the limitations that naturally arise of the constrained optimization problem, a supervisory-cascaded control is proposed.

The stability of the supervisory modes are discussed and efficiency of the proposed robust control it is shown through numerical simulation. It is shown that the more strict restrictions on the power change of the FC leads to more sensibility of optimized-based strategy to uncertainty, motivating the use of alternative, possible heuristic, EMS for these cases.

References

[1] A. Khaligh and Z. Li (2010). "Battery, ultracapacitor, fuel cell, and hybrid energy storage systems for electric, hybrid electric, fuel cell and plug-in hybrid electric vehicles: state of art" IEEE Trans. Vehicular, Vol. 59, No. 6, pp 2806-2814.

[2] H.-C.B. Jensen, E. Schualtz, P.S. Koustrup, S.J.Andreasen and S.K.Kaer (2013). "Evaluation of fuel cell range extender impacto on hybrid electrical vehicle perfomance" IEEE Trans. Vehicular, Vol. 62, No. 1, 2013, pp 50-60.

[3] A. Emadi, K. Rajashekara, S. S. Williamson and S. M. Lukic (2005)."Topological overview of hybrid electric and fuel cell vehicular power system architectures and configurations" IEEE Trans. Vehicular, Vol. 54, No. 3, pp 763-770.

[4] D. Feroldi, M. Serra and J. Riera (2009). "Energy management strategies based on efficiency map for fuel cell hybrid vehicles" J. Power Sources, Vol. 190, pp 387-401.

[5] D. Feroldi, M. Serra and J. Riera (2009). "Design analysis of fuel-cell hybrid system oriented to automotive applications" IEEE Trans. Vehicular, Vol. 58, No. 9, 2009, pp 4720-4729.

[6] B. Geng, J.K.Mills and D. Sung (2012). "Two-stage energy management control of fuel cell plug-in hybrid electric vehicles considering fuel cell longevity" IEEE Trans. Vehicular, Vol. 61, No. 2, pp 498-508.

[7] E. Tazellar, B. Veenhuizen, P. van den Bosch and M. Grimminck (2012). "Analytical solution of the energy management for fuel cell hybrid propulsion systems" IEEE Trans. Vehicular, Vol. 61, No. 5, 2012, pp 1986-1998.

[8] A. Ravey, B. Blunier and A. Miraoui (2012)."Control strategies for fuel cell based hybrid electric vehicles: from offline to online and experimental results" IEEE Trans. Vehicular, Vol. 61, No. 6, 2012, pp 2452- 2457.

[9] W.L. Brogan (1991)."Modern Control Theory" Prentice Hall, N.J.

[10] E. D. Sontag (1998)."Mathematical Control Theory. Deterministic Finite Dimensional Systems" Springer N.Y.

[11] S.Kelouwani, N. Henao, K.Agbossou, Y. Dube and L. Boulon (2012). "Two-layer energy-management architecture for a fuel cell HEV using road trip information" IEEE Trans. Vehicular, Vol. 61, No. 9, pp 3851-3864.

[12] W. Na, T. Park, T. Kim and S. Kwak (2011). "Light fuel-cell hybrid electric vehicles based con predictive controllers" IEEE Trans. Vehicular, Vol. 60, No. 1, pp 89-97.

[13] E. Schaltz, A. Khalilgh and P.O.Rasmussen (2009). "Influence of battery/ultracapacitor energy-storage sizing on battery lifetime in a fuel cell hybrid electric vehicle" IEEE Trans. Vehicular, Vol. 58, No. 8, pp 3882-3891.

[14] S.S. Williamson and A. Emadi (2005). "Comparative assesment of hybrid electric and fuel cell vehicles based on comprehensive well-to-wheels efficiency analysis" IEEE Trans. Vehicular, Vol. 54, No. 3, pp 856-862.

[15] C.C. Chan, A. Bouscayrol and K. Chen (2010). "Electric, hybrid and fuel cell vehicles: architectures and modeling" IEEE Trans. Vehicular, Vol. 59, No. 2, pp 589-598.

[16] A. Ravey, N. Watrin, B. Blunier, D. Bouquain and A. Miraoui (2011). "Energy-source-sizing methodology for hybrid fuel cell vehicles based on statistical description of driving cycles" IEEE Trans. Vehicular, Vol. 60, No. 9, pp 4146-4174.

[17] P. Thounthoung, V. Chunkag, P. Sethakul, B. Davat and M. Hinaje (2009). “Comparative study of fuel cell vehicle hybridization with battery or supercapacitor storage device” IEEE Trans. Vehicular, Vol. 58, No. 8, 2009, pp 3892-3904.

[18] Y. Wu and H. Gao (2006). “Optimization of fuel cell and supercapacitor for fuel cell electric vehicles” IEEE Trans. Vehicular, Vol. 55, No. 6, pp 1748-1755.

[19] I. Cervantes, J. Morales-Morales, I.A. Diaz-Diaz and A. Mendoza-Torres (2011). “Switched control for power management in hybrid propulsion schemess” IEEE Vehicular Power and Propulsion Conference, Chicago Illionois.

[20] M.A. Hanson (1981). “On sufficiency of the Kuhn-Tucker conditions” Journal of Mat. Anal. Appl., Vol. 80, pp 545-550.

[21] I. Cervantes, A. Mendoza-Torres, A. Emadi and I. A. Diaz-Diaz (2013). “Robust Switched Current control of convertes” to appear IET Control theory and applications.

[22] J. Bernard, S. Delprat, F. N. Büchi and T. M. Guerra (2009). “Fuelcell hybrid powertrain: Toward minimization of hydrogen consumption, IEEE Transactions on Vehicular Technology, Vol. 58 No. 7, p.p. 3168-3176